



NEW EMPIRICAL DESIGN PRACTICE TO EVALUATE THE SEALING CAPABILITY OF SPLIT FLANGE FOR STEAM TURBINE

Enrico Giusti

BHGE (Turbomachinery & Process Solutions)
Nuovo Pignone Tecnologie SRL, Florence, Italy

Alessandro Giorgetti, Andrea Girgenti, Gabriele Arcidiacono

Department of Innovation and Information Engineering
G. Marconi University, Rome, Italy

Damaso Checcacci, Walter Schiavi

BHGE (Turbo machinery & Process Solutions)
Nuovo Pignone Tecnologie SRL, Florence, Italy

ABSTRACT

In the oil and gas industry, machines and equipments usually operate in harsh and tough service conditions due to the exposure at high temperatures and pressures, as well as mechanical loads. In this context, operators' safety in operating machines shall be granted, notwithstanding the adoption of new design criteria due to cost reduction and new operative conditions. While Finite Element Analyses allow the simulation of working stresses and deflections accurately, these results need to be compared with experimental data in order to identify conditions which correspond to leakages in turbine horizontal split flanges. This paper proposes a new design criterion that permits to verify the sealing capability of metallic butt joints undergoing high temperatures and pressures using the results of Finite Element Analysis. This criterion is based on experimental data, collected through the simulation of extreme service conditions at which sealing failures occur.

Keywords: sealing, steam turbines, FEA, design practice, flanges.

Cite this Article: Enrico Giusti, Alessandro Giorgetti, Andrea Girgenti, Gabriele Arcidiacono, Damaso Checcacci and Walter Schiavi, New Empirical Design Practice to Evaluate the Sealing Capability of Split Flange for Steam Turbine, International Journal of Mechanical Engineering and Technology 9(2), 2018. pp. 839–850.
<http://www.iaeme.com/IJMET/issues.asp?JType=IJMET&VType=9&IType=2>

1. INTRODUCTION

Equipments and machine components for oil and gas applications are usually exposed to severe operative conditions, since the oilfield sites are increasingly located in remote places with extreme environments. This reason makes the design and the economic sustainability of machines, as well as its components, more and more challenging [1]. These difficulties are even more critical since mechanical components shall be able to ensure both their reliability and the safety of operators. On the other hand, periods with a lower oil price and a major attention at the capital expenditures (CapEx) require the further lowering of machines cost, which can be achieved through the characterization of new materials, the increase in expensive components lifetime [2] and the definition of new design criteria.

The characterization of material strength for a large number of service conditions and the definition of their employability boundaries (especially in acidified environments) are key issues in the oil and gas industry [3, 4]. Many techniques can be found in literature to improve techniques for investigating boundaries of the material safe service [5, 6]. On the other hand, the design of reliable, efficient machines, e.g. steam turbines, requires the application of many diverse areas of technology [7]. There are many competing designs and material requirements that must be thoroughly evaluated in order to achieve optimum trade-offs. In this context, the definition of new design criteria and new principles to verify the functionality of components in critical conditions and achieve better designs is a complex task, which requires a better understanding of the physical behavior of involved phenomena in machine operations. The design of horizontal split flange within steam turbines has to take account of this issue. In fact, this component shall be able to avoid hot steam leakages, ensuring the proper sealing effect, thus the evaluation of its functionality results very difficult, needing a deep comprehension of contact phenomena at the interface.

The simulation of the contact among bodies has a great importance in many industrial applications, which is why various attempts to solve this problem can be found in several fields [8-10]. Many studies have dealt with the simulating of contact between two surfaces, both analytically [11] and numerically [12]. On the other hand, the practical simulation of contact problems is computationally difficult, mainly because the boundary conditions of the considered bodies depend on many variables [13, 14]. Only a few problems can be solved analytically; when the contacting bodies have complex geometries, numerical methods have to be applied. The mechanical behavior in the contact interface can be modelled through Finite Element Analyses (FEA) according to the two following methods [12]: a non-penetration condition as a purely geometrical constraint or the development of constitutive micromechanical laws.

The first case relates the contact pressure to the reaction in the contact area and calculates it through the constraint equation. The latter obtains constitutive equations for the normal contact investigating the micromechanical behavior within the contact surface. The micromechanical behavior depends on material parameters like the hardness, geometry and roughness, but its simulation is very complex; therefore, the models are only meant to reproduce the main phenomena, assuming either an elastic or a plastic deformation of the asperities being in real contact in the interface. The modelling of the frictional response, i.e. the interfacial behavior in the tangential direction, is even more difficult and is treated in many ways by researchers [15], like trying to formulate a third body at the interface which has special properties and is only present when the tangential mechanical load is applied [16].

The weak formulation of contact problems models the contact conditions as inequality constraints. The numerical solution of these problems is applied in combination with

Lagrangian multiplier or penalty techniques [17, 18]; most standard finite element codes which are able to handle contact problems use one of these two methods [13].

Some studies, focus on the design of the horizontal split flange for steam turbines, taking into account many factors that affect the contact. Traupel [11] relates the tightening of the studs, compressing one flange against the other with a parameter to characterize the contact between the two surfaces (such as the contact pressure). Notwithstanding the capability to successfully explain how the mechanical system works, such theories do not provide any threshold criterion for evaluating the sealing capability of the joint, since it depends on both the manufacturer experience and the specific application.

The horizontal split flange is a metallic butt joint that works with high pressures and temperatures, thus being subjected to creep phenomena. A similar joint provides the sealing effect until the contact pressure between the two compressed surfaces, given by the studs' preload, is not zeroed. If the internal gas pressure, which tends to separate the two contact surfaces of the compressed flange, grows up until it zeroes the contact pressure, the joint fails and the hot vapor leaks out the outer turbine case, putting at risk operators' safety. Figure 1 shows the radial section of the joint, outlining the effect of the internal service pressure which, in opposition to the contact pressure, tends to separate the two surfaces of the joint.

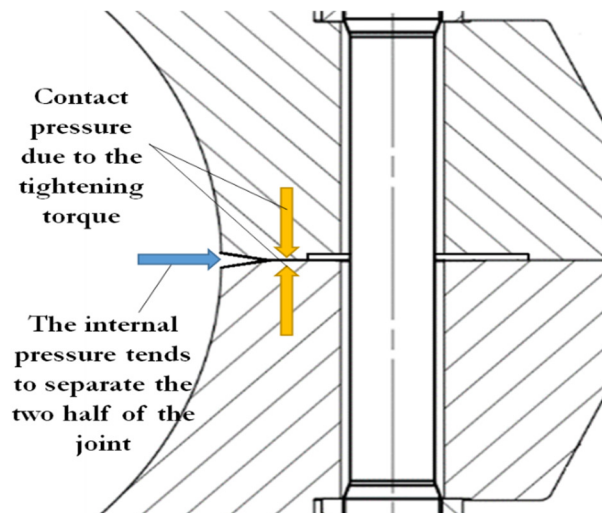


Figure 1 Effect of internal service pressure against the contact pressure at the interface of the joint

The sealing capability of the joint changes over time due to material's relaxation, produced by creep at high temperatures. The relaxation determines a reduction of the bolts' preload, thus the reduction of the contact pressure at the joint interface. In order to identify a robust criterion to assess the joint sealing capability that is reliable over time, this phenomenon shall be taken into account, performing experiments with reduced tightening torques with respect to the nominal one (usually considered as 75% of the bolt yield strength). The economical product life depends on the duration, which corresponds to an acceptable joint sealing capability, as a function of the service conditions in terms of pressure and temperature. The relaxation phenomenon can be modelled through the estimated studs preload that is needed in order for the turbine to reach the major service inspection, which is when the machine is stopped, and the joints are replaced with new ones. Obviously, the numerical calculation of this effect shall include uncertainties in accounting various effects, e.g. the preload allowance of the tightened studs, the different behaviour of material from the supposed one and also the knowledge of the exact time of the relaxation.

The contact between the two flanges, from which derives the sealing capability of the joint, can be expressed through both the contact pressure and the extension of the contact

interface. In fact, during the regular service of the turbine outer case, the flanges present an extent of the contact interface where contact pressure is applied, although opposed by the fluid internal one. On the other hand, if the contact between the two case halves finishes, the results are a leakage and no more the contact pressure is applied.

The extension of the contact interface (see Figure 2) can be measured as the minimum radial distance between flange inner diameter and the threaded holes (named “path”). The contact path could be defined in millimetres or as percentage of the path.

The forces at the contact interface can be derived deterministically or numerically as a function of the extension of the contact interface, the studs preload and the internal fluid pressure.

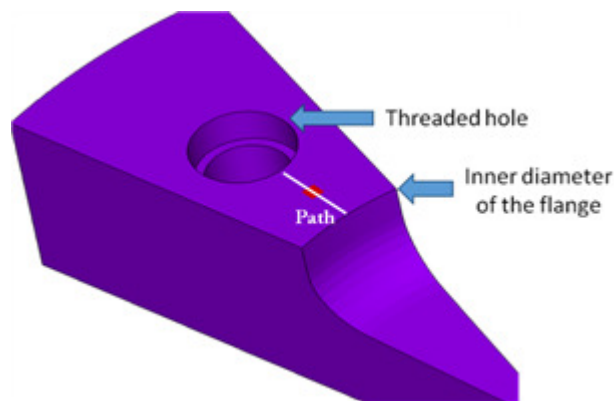


Figure 2 A portion of the flange with the definition of the “path”: the minimum radial distance between flange inner diameter and the threaded holes

The numerical analysis performed by means of Finite Elements Method (FEM) allows to appreciate how the contact conditions vary due to the application of different external loads. When two distinct surfaces get in contact, they are tangent but not to penetrate each other. Furthermore, the two surfaces can transmit just normal compression forces and friction shear ones. The overall system stiffness depends on the state of contact and the finite element model shall set a relationship between the surfaces in order to avoid their penetration; such condition is called “contact compatibility” [19].

The contact condition is modelled according to the scheme in Figure 3, where the normal force (F_n) produces the penetration in the normal direction (x_p).

The contact constraint between the two surfaces is defined through the normal stiffness of contact elements (FKN) parameter through (1), representing the relation among the three parameters F_n , x_p and FKN:

$$F_n = FKN \cdot x_p \quad (1)$$

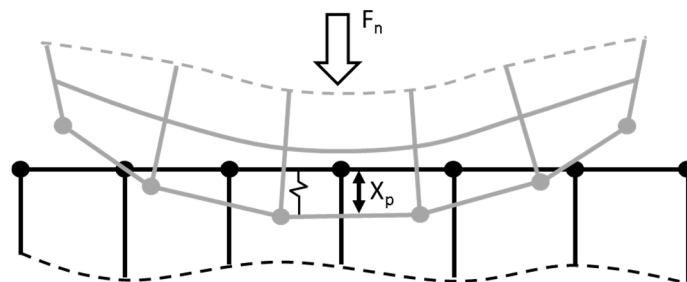


Figure 3 Representation of the contact model between two surfaces

Given a certain F_n , x_p tends to be zero as FKN tends to infinity, hence a high value for the normal stiffness is more realistic, despite it can make more difficult for the solution of the model. In fact, difficulties in solving the model may depend on the chattering condition, that occurs when an element literally bounces back on the other due to high stiffness [20]. Repeated simulations show different extents of the contact surface depending on the variation of FKN, leading to different results, like those shown in Figure 4. The contact path for evaluating the capability of the sealing in the split flanges is a not reliable variable due to different results obtained as a function of the chosen normal stiffness (FKN).

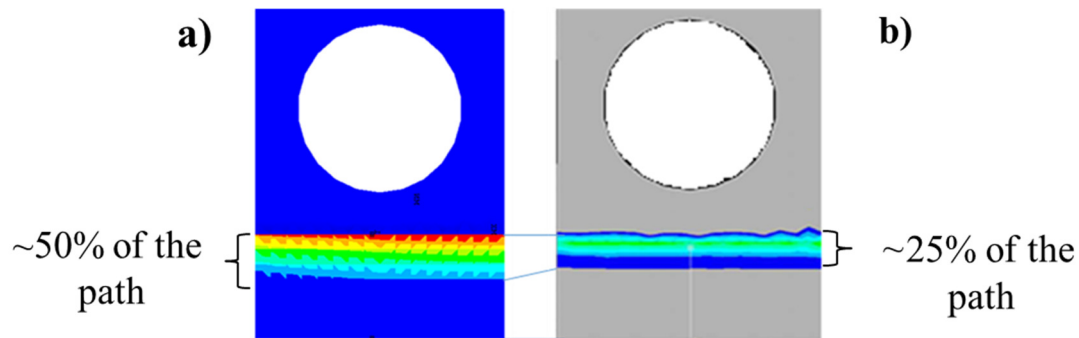


Figure 4 Different percentages of calculated contact path according to the contact criterion, after 50,000 hours and assuming the FKN equal to 0.01 (a) or the FKN equal to 1 (b)

Notwithstanding many techniques are available to calculate (deterministically or numerically) the contact pressure or surface between two flanges in various service conditions [11], the designer needs criteria to verify the sealing capability of the horizontal split joint, ensuring both reliability of the sealing capability and cost reduction. These criteria shall be accurately customized and developed for a given specific application, basing them on experimental evidence [21, 22]. Although the simulation of working conditions is accurately executed through FEA, the conditions which correspond to sealing failures should be experimentally verified as well, in order to spot criteria to verify the sealing capability of split flanges. In particular the steam turbine outer case works like a pressure vessel that treats a high temperature fluid; thus, the simulation of the contact at the interface between its two halves, as well as the consequent definition of a criterion to evaluate the sealing efficacy, shall be verified experimentally in order to obtain a reasonable safety margin and reduced costs at the same time.

This paper studies the relation sealing capability obtained by experimental tests vs contact path calculated by FEA analysis. Moreover 2 design criteria to verify the sealing capability of the split flanges between the two parts of the steam turbine outer case will be introduced and discussed.

2. THE MATERIAL AND METHOD

Some experimental tests have been made to analyze the relationship between FEA results and the real sealing capability of the joint. In particular FEM calculates the contact path as a function of internal pressures, assuming the studs tightening torque and the surfaces features as constants, including FKN. In particular the experiments aim at measuring the internal fluid pressure which corresponds to a leakage, i.e. a sealing failure. The experiment consists of increasing the internal pressure within a dummy vessel, until a leak occurs. The service temperature, the joint geometry and the studs preload are kept constant to ease the experimental reproducibility. The dummy vessel has the similar geometry to a turbine horizontal split flanges by GE. The studs size and type are the same of the original joint as

well as their number and spacing. A similar device is simpler to pressurize than a whole turbine and allows the reproduction of the joint behavior with an internal pressure. The dummy pressure vessel is cylindrical shaped, composed of two flanged halves that are joined through studs (Figure 5a). The necessary hollowness to hold the pressurized fluid is shaped in each single half, working when the vessel is closed, and studs are tightened at a predefined % of the bolt yield strength. The internal service pressure is reached pumping oil inside the cavity. The relative choice of an incompressible fluid is suggested to identify easily the leakages and to simplify the experiment.

The vessel is mounted within a circuit to pump the oil inside, and measure both the internal pressure and the stud elongations under load (Figure 5b and 5c). The circuit pressure is measured by a gauge, while the pressure inside the vessel is measured through a transducer. Stud elongations under load are measured through a dial gauge on their free upper end.

Since the tightening preload tends to loosen over time due to the material relaxation or the presence of thermal loads, executing room temperature experiments with reduced tightening torques is useful to take into account this phenomenon in a controlled way. Three experimental campaigns are executed, each with different tightening torques, to outline different system behaviours due to the material relaxation phenomenon and assess the criterion robustness. The three campaigns present tightening torques respectively equal to 70%, 52% and 35% of the bolts yield strength and count five runs each one.

The experimental procedure sets that, as a first step, the flat flanged surfaces which become in contact are degreased using a solvent. The seal between the two flanges consists of Arexons paste, which allows to polymerize at room temperature and is applied to the lower flange. Thus, the vessel is closed, and all the sixteen screws are tightened with one of the three tightening torques. The tightening process involves groups of studs according to a cross pattern, which is useful to avoid the bending of the flanges. The tightening torque is applied by a hydraulic jack through two phases of the process:

1. half of the desired value of each campaign;
2. all the desired value of each campaign.

The stud elongations are measured by a dial gauge for spotting the eventual loosening due to the tightening of the other studs.

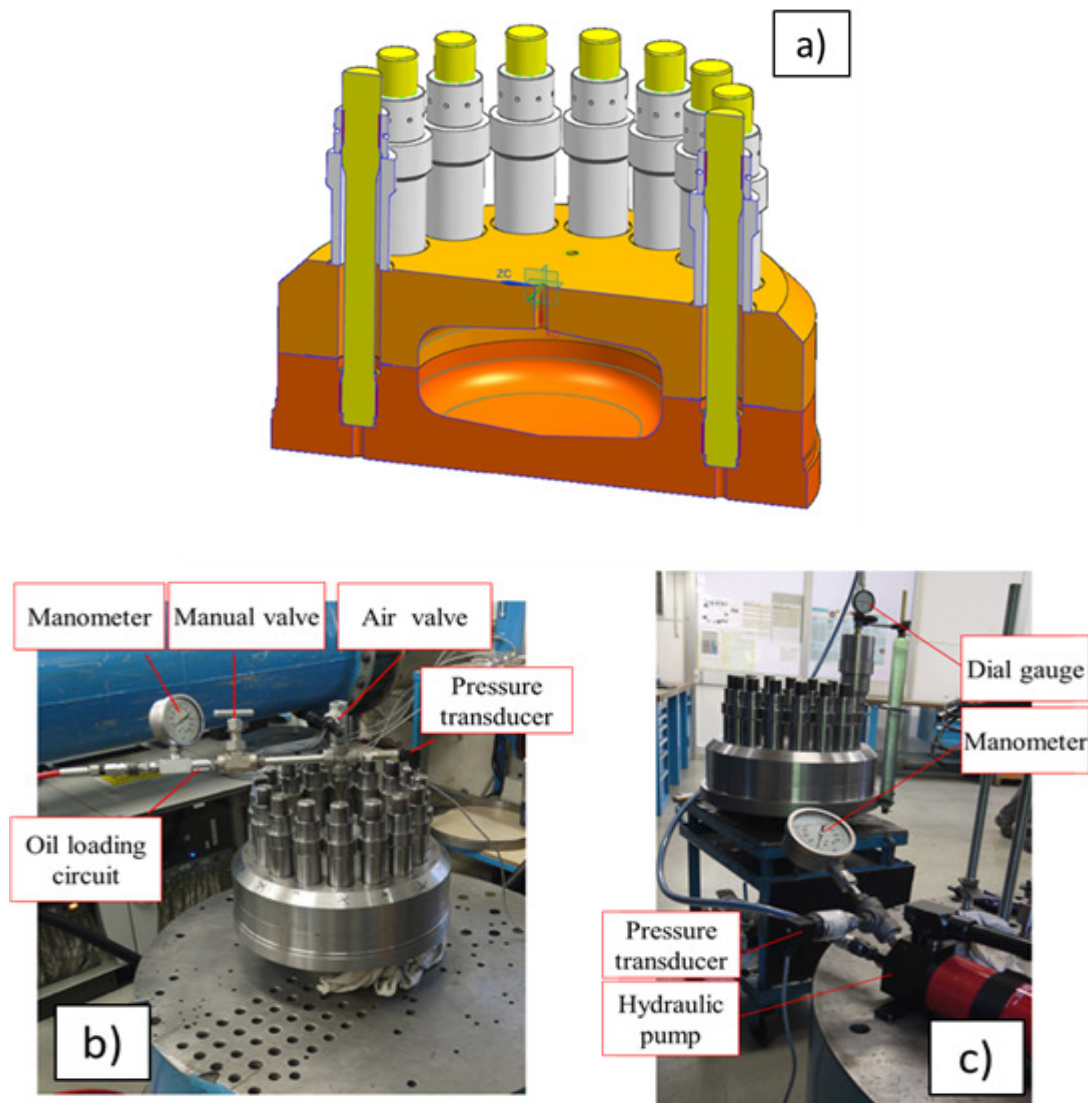


Figure 5. Image copyright 2017 General Electric Company or its affiliates. Used by permission. a) Radial section of the dummy vessel, b) Detail of the last section of the loading circuit which brings pressurized oil inside the vessel, c) Another detail of the first part of the circuit with the pump to pressurize oil. A dial gauge is also mounted to measure the stud elongation

The measures of stud elongations using the tightening torque at 35%, 52% and 70% of the bolt yield strength (Y_s) are listed in Table 1.

The ratio between the standard deviation and the average for each run are unlikely repeatable, since a different amount of lube on threads is enough to obtain a different friction coefficient and, consequently, a different applied load on the stud. On the other hand, an error in applying the tightening torque to a single screw is likely not responsible for an eventual leakage, since the load tends to share out on the other studs. The use of hydraulic jacks to apply torques has brought standard deviations [23] in elongations with a 10^{-2} mm magnitude. This can be considered a very good result, thus allowing to neglect errors due to the studs tightening as a first approximation.

The ratio between the standard deviation and the average for each run are unlikely repeatable, since a different amount of lube on threads is enough to obtain a different friction coefficient and, consequently, a different applied load on the stud. On the other hand, in the

analysed configuration, an error in the tightening torque of a single screw could be counterbalanced by sharing the load among many studs.

Once the vessel is closed and the studs are tightened, the hollowness is filled with oil and eventual air bubbles are left to blow out from the system. After the pump and the instruments are connected, the system is ready to be pressurized.

Table 1 Elongation values in mm of studs due to their tightening in different experimental campaigns

Stud #	Test (1)					Test (2)					Test (3)				
	Tightening torque 35% Ys					Tightening torque 52% Ys					Tightening torque 70% Ys				
1	0,25	0,28	0,25	0,26	0,24	0,42	0,43	0,43	0,50	0,48	0,57	0,6	0,61	0,63	0,60
2	0,23	0,24	0,26	0,22	0,26	0,43	0,42	0,42	0,48	0,43	0,53	0,56	0,58	0,65	0,60
3	0,24	0,25	0,3	0,25	0,24	0,44	0,42	0,42	0,46	0,46	0,58	0,6	0,58	0,60	0,59
4	0,25	0,23	0,28	0,26	0,25	0,40	0,40	0,42	0,46	0,48	0,62	0,58	0,58	0,59	0,59
5	0,25	0,26	0,24	0,23	0,28	0,41	0,42	0,44	0,44	0,49	0,53	0,59	0,31	0,63	0,58
6	0,22	0,22	0,25	0,21	0,24	0,43	0,44	0,41	0,45	0,46	0,54	0,57	0,59	0,60	0,58
7	0,24	0,21	0,23	0,25	0,28	0,39	0,41	0,44	0,47	0,42	0,54	0,6	0,56	0,60	0,59
8	0,23	0,22	0,22	0,25	0,26	0,39	0,43	0,42	0,47	0,26	0,59	0,58	0,56	0,60	0,57
9	0,26	0,22	0,23	0,24	0,22	0,42	0,43	0,45	0,53	0,46	0,62	0,61	0,61	0,60	0,59
10	0,24	0,24	0,22	0,24	0,23	0,45	0,44	0,44	0,51	0,46	0,54	0,59	0,57	0,60	0,61
11	0,23	0,22	0,24	0,25	0,26	0,44	0,41	0,44	0,45	0,46	0,62	0,60	0,59	0,62	0,57
12	0,22	0,24	0,28	0,22	0,24	0,43	0,39	0,42	0,47	0,47	0,57	0,59	0,58	0,58	0,57
13	0,26	0,28	0,23	0,25	0,24	0,42	0,41	0,43	0,44	0,46	0,54	0,60	0,61	0,63	0,57
14	0,22	0,23	0,22	0,22	0,26	0,46	0,41	0,45	0,45	0,43	0,59	0,61	0,61	0,60	0,57
15	0,24	0,24	0,23	0,25	0,24	0,51	0,41	0,43	0,47	0,46	0,57	0,57	0,60	0,57	0,57
16	0,25	0,23	0,22	0,25	0,24	0,43	0,39	0,44	0,43	0,43	0,57	0,57	0,57	0,59	0,57
AVG.	0,24	0,24	0,24	0,24	0,25	0,43	0,42	0,43	0,47	0,44	0,57	0,59	0,57	0,61	0,58
ST. DEV.	0,013	0,021	0,025	0,016	0,017	0,029	0,015	0,012	0,027	0,053	0,032	0,016	0,071	0,021	0,013

Table 2 Measured values for pressures corresponding to the leakage for the five runs for each tightening torques

	Test (1)					Test (2)					Test (3)				
	Tightening torque 35% Ys					Tightening torque 52% Ys					Tightening torque 70% Ys				
Leaking Pressure	260	242	235	242	237	425	412	381	428	402	490	490	515	495	500
AVG.	243,2					409,6					498				
ST.DEV.	9,88					19,09					10,37				

The internal fluid pressure is gradually (10 bar-step) incremented and a transient period of few minutes able to measure the regime behaviour. The gradual increment of the internal pressure is useful to spot the value when a visible leakage occurs, according to Figure 6. The pressure curve shows flat increments to a higher value due to the pumping of further oil within the vessel cavity. A sealing instability prevents the massive leakage and occurs when the curve of pressure changes in slope, decreasing. Then a further insertion of oil causes a drastic fall of pressure and the consequent leakage.

The internal pressure values, which correspond to the leakage, are reported in Table 2 for each run in all the 3 campaigns. Data are summarized through their averages and standard

deviations to perform a statistical analysis as already done in more detail by the authors in other research activities [23].

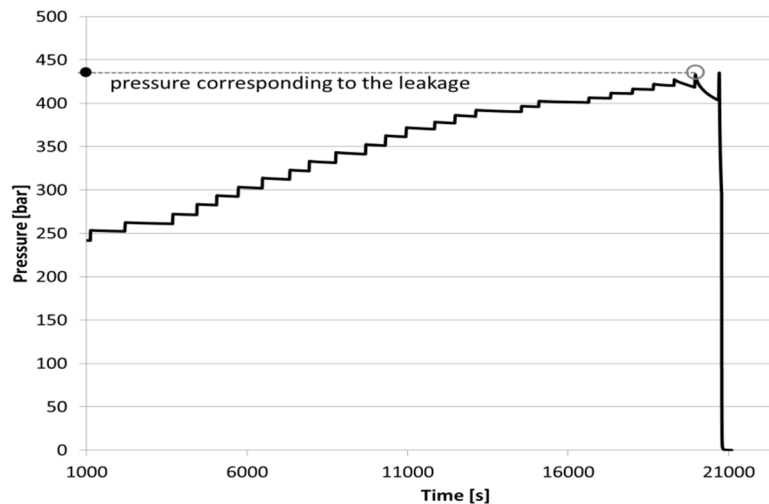


Figure 6 Pressure increments till a leakage is visible and the seal failure occurs

3. RESULTS AND DISCUSSION

The introduction of a new criterion to verify the sealing capability is affected by several uncertainties depending on parameters in numerical models rather than the definition of sealing failure: for this reason, it needs to be assessed through experimental outcomes (for example: entering the fluid internal pressure which corresponds to a sealing failure allows the definition of evaluation criteria for sealing capability, that is based on the amount of contact path). From the numerical modelling standpoint, the contact conditions in terms of contact path depend on the tightening torque, the internal pressure and the interface normal stiffness. Figure 7 shows the three simulated curves which link the contact path to the pressure values, applying a tightening torque of 52% of the stud yield strength. The simulations point out a similar behavior using FKN values greater than 1 (1 and 10), while a reduced value (FKN=0.01) requires a higher pressure to reduce the same percentage of contact path. The dashed line marks the 50% of the contact path, that is reached with an internal pressure of 420, 428, 480 and 620 bar for FKN equal respectively to 10, 1, 0.1 and 0.01. The similar behavior of curves with FKN greater than 1 shows that, in this case, the elements normal stiffness does not affect the result. As an addition, calculated penetrations at the interface result less than 10-3 mm for these FKN values, hence making them preferable for calculating the contact path by FEM.

Figure 8 shows the calculated length of the contact path, where the pressure at the interface is parametrized as k_p times the internal pressure ($k_p=1$ means absence of safety factor as the contact pressure is equal to inner pressure). The 3 curves are calculated as functions of the internal pressure for different tightening torques to take into account the effect of the material relaxation over time. The variation of the leaking pressure, represented by its average and relative range, defines a corresponding interval of values on the length.

Considering this relationship, it is possible to define a design criterion as follows: the sealing capability of the flange is assured at a specific internal pressure if the contact pressure on the contact path is at least k_p times (k_p to be assumed between 1,5 and 10 depending on type of service, type of sealing surface shape and roughness) the internal maximum pressure for at least a length L_c :

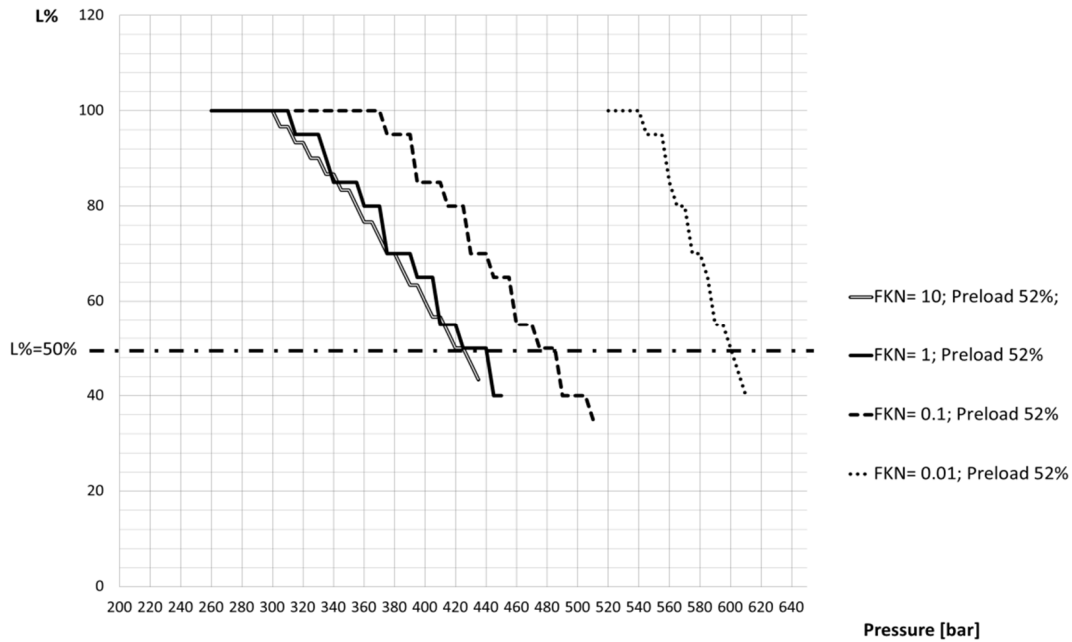


Figure 7 Percentage of contact path ($L\%$) as a function of the internal pressure: the curves are calculated with three different values of FKN and the same tightening torque

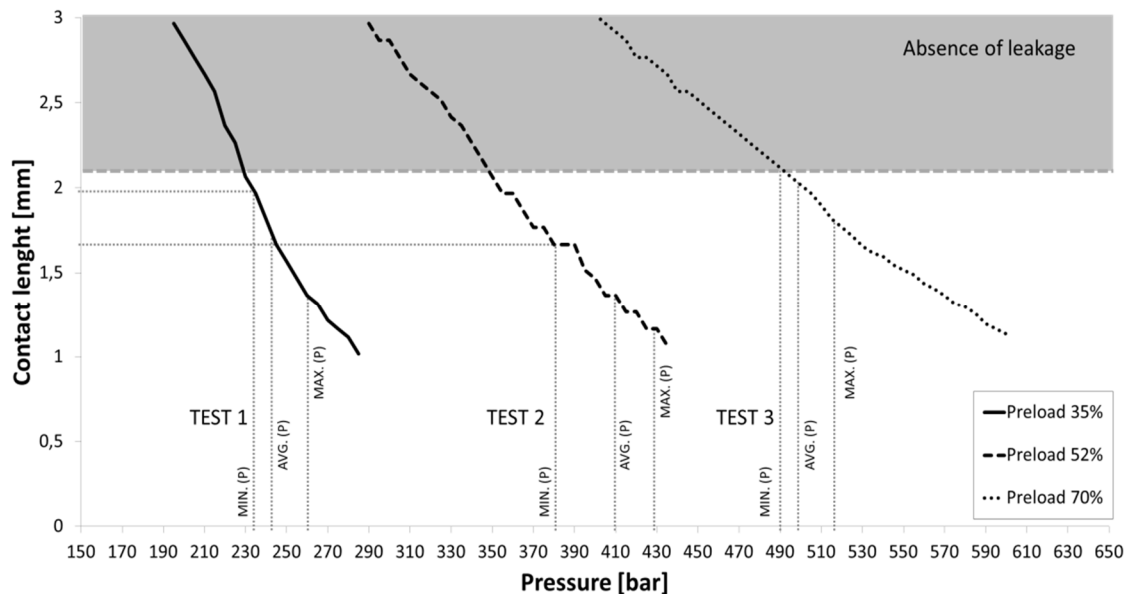


Figure 8 Calculated values of contact length (mm) corresponding to the effective leaking pressure (FKN=10)

The threshold value for L_c to be adopted for this criterion is set by the highest length that corresponds to the minimum value of leaking pressure; thus, according to Figure 8, L_c to avoid the seal failure should be at least 2,1mm. Then the designer can increment this value using a safety factor ($k_{L_c} > 1$) in order to consider the uncertainties relative to the specific operating condition of the turbine and the sealing surface condition.

In particular, the proposed criteria present some advantages:

- It permits to use easily FEM results to select the correct dimensions of the flange;
- It is based on experimental results;
- It can be used with different tightening torques and it can consider the effect of the creep phenomenon over time;
- It is function of the internal pressure used in the FEM analysis.

5. CONCLUSIONS

The topic of simulating contact conditions has been dealt by many authors through various techniques. The complexity of deterministic approaches developed thanks to the diffusion of computers and the improvements in FEA have determined nowadays the simulation of contact conditions mainly through numerical models. However, the accurate simulation of contact conditions is not enough to evaluate the sealing capability of joints. Seals are widely used in many mechanical applications and may undergo severe working conditions like, for example, metallic butt joints in steam turbines that work with high pressures and temperatures. This paper introduces a design criterion useful to evaluate the proper working of the seal. The criterion has been developed using an empirically approach. In particular some sealing capability tests have been executed on a pressure vessel which reproduces the real joint geometry and service condition of the system. The vessel is gradually pressurized with oil till a leakage occurs. The material relaxation due to high temperature exposure over time is reproduced through repeated campaigns with reduced tightening torques for studs. The experiments aim at measuring pressures which correspond to sealing failures, in order to calculate the corresponding contact path at the interface through FEM. The criterion sets a minimum length in the contact interface where the pressure is equal to k_p times the internal value. The criteria can be used to verify the sealing capability in very extreme conditions, like those in steam turbines, and are validated through experimental data, thus providing a reliable reference for the designer. Ongoing future works will investigate the effect of the uncertainties about working conditions, like the effective material behavior, the surface roughness, the error in the tightening torque of a single screw and the typology of seal used.

REFERENCES

- [1] Yanagihara K., Miura H., Nishida H., et al. Verification of Performance and Operating Characteristics of High Pressure Gas Injection Centrifugal Compressor. ASME Turbo Expo: Power for Land, Sea, and Air, Volume 9: Oil and Gas Applications; Supercritical CO2 Power Cycles; Wind Energy: V009T24A019, 2015.
- [2] Monti C., Giorgetti A., Tognarelli L., Mastromatteo F. On the Effects of the Rejuvenation Treatment on Mechanical and Microstructural Properties of IN-738 Superalloy. Journal of Materials Engineering and Performance, 26(5), 2017, pp. 2244-2256.
- [3] Venezuela J., Liu Q., Zhang M., Zhou Q., Atrens A. A review of hydrogen embrittlement of martensitic advanced high-strength steels. Corrosion Reviews, 34(3), 2016, pp. 153-186.
- [4] Zhao W., Zou Y., Matsuda K., Zou Z. Corrosion behavior of reheated CGHAZ of X80 pipeline steel in H₂S-containing environments. Materials and Design, 99, 2016, pp. 44-56.
- [5] Girgenti A., Giorgetti A., Anselmi M., Scatena A. Improvement of the test equipment for a stress corrosion lab through the Axiomatic Design. Procedia CIRP, 34, 2015, pp. 162-167.

- [6] Girgenti A., Giorgetti A., Citti P., Romanelli M. Development of Custom Software for Processing the Stress Corrosion Experimental Data through Axiomatic Design. *Procedia CIRP*, 34, 2015, pp. 250–255.
- [7] Al-attab K.A., Zainal Z.A. Externally fired gas turbine technology: A review, *Applied Energy*, 138, 2015, pp. 474-487.
- [8] Hantouche G., Kukreti A.R., Rassati G.A., Swanson J.A. Modified stiffness model for thick flange in built-up T-stub connections. *J. Constr. Steel Res.*, 81, 2013, pp. 76–85.
- [9] Tsalkatidis T., Avdelas A. The unilateral contact problem in composite slabs: Experimental study and numerical treatment. *J. Constr. Steel Res.*, 66, 2010, pp. 480–486.
- [10] Nelson N.R., Prasad N.S., Sekhar A.S. Finite element analysis of flange joint with single and twin gaskets under external bending load, American Society of Mechanical Engineers, Pressure Vessels and Piping Division (Publication) PVP, Vol. 2, ASME 2015 Pressure Vessels and Piping Conference, PVP 2015; Code 117787, 2015.
- [11] Traupel W. *Thermische Turbomaschinen*, Springer Berlin Heidelberg, Berlin, 2001.
- [12] Wriggers P. Finite element algorithms for contact problems *Arch. Comput. Methods Eng.*, 2, 1995, pp. 1–49.
- [13] De Lorenzis L., Wriggers P., Weißenfels C. Computational Contact Mechanics with the Finite Element Method. *Encyclopedia of Computational Mechanics Second Edition*. 1: pp. 1–45, 2017.
- [14] Zhong Z., Mackerle J. Contact-Impact Problems: A Review with Bibliography. *ASME. Appl. Mech. Rev.*, 47(2), 1994, pp. 55-76.
- [15] Duvant G., Lions J. *Inequalities in mechanics and physics*, Springer-Verlag, 1976.
- [16] Kragelsky I., Shchedrov V., *Development of the Science about Friction*, Moscow, 1956.
- [17] Gafni E.M., Bertsekas D.P. Two-Metric Projection Methods for Constrained Optimization. *SIAM J. Control Optim.*, 22, 1984, pp. 936–964.
- [18] Luenberger D. *Linear and nonlinear programming*, Kluwer Academic Publishers, 2008.
- [19] Bathe K.J., Bouzinov P. On the constraint function method for contact problems. *Comput. Struct.*, 64, 1997, pp. 1069–1085.
- [20] Abdullah O., Schlattmann J., Al-Shabibi A.M. Stresses and deformations analysis of a dry friction clutch system. *Proceedings 13th Int. Conf. Tribol.*, Kragujevac, Serbia, 2013.
- [21] Ma K., Zhang Y., Zhang L., Guan K. Behavior of bolted joints with metal-to-metal contact type gaskets under bolting-up and loading conditions”, *Proceedings of the Institution of Mechanical Engineers, Part E: Journal of Process Mechanical Engineering*, 230(4), 2016, pp. 284-291.
- [22] Abid M. Determination of safe operating conditions for gasketed flange joint under combined internal pressure and temperature: A finite element approach. *Int. J. Press. Vessel. Pip.*, 83(6), 2006, pp. 433–441.
- [23] Arcidiacono G., Calabrese C., Yang K. *Leading Processes to Lead Companies: Lean Six Sigma: Kaizen Leader & Green Belt Handbook*. Milan, Italy: Springer Verlag, 2012.
- [24] Arcidiacono G., Berni R., Cantone L., Placidoli P. Kriging models for payload-distribution optimization of freight trains. *International Journal of Production Research*, 55(17), 2017, pp. 4878-4890.
- [25] Chelamalasetti Pavan Satyanarayana and Dr YV Hanumantha Rao, Design and Analysis of High-Pressure Casing of A Steam Turbine. *International Journal of Mechanical Engineering and Technology*, 8(7), 2017, pp. 11–16.